ISSN 0010-9525, Cosmic Research, 2015, Vol. 53, No. 3, pp. 171–181. © Pleiades Publishing, Ltd., 2015.
Original Russian Text © A.V. Biryukov, 2015, published in Kosmicheskie Issledovaniya, 2015, Vol. 53, No. 3, pp. 183–194.

Test Results of Radio Interferometer with Zero Base in the RadioAstron Project

A. V. Biryukov

Astro Space Center P.N. Lebedev Physical Institute, Russian Academy of Sciences, Moscow, Russia
e-mail: biriukov@asc.rssi.ru

Received November 18, 2014

Abstract—In preparation for the launch of a space telescope for ground tests within the ground–space RadioAstron project, procedures and methods are developed in order to carry out tests under the zero base interferometer mode, which will make it possible to measure complex parameters of the onboard arm of the space–ground very-long-baseline radio interferometer that determine its basic parameter, i.e., sensitivity.

DOI: 10.1134/S001095251503003X

1. INTRODUCTION

The development of the scientific equipment (SE) for the space–ground radio interferometer was a fundamentally new technical challenge, both in radio astronomy and in space device engineering. The fulfillment of standard requirements for space equipment is greatly complicated by the requirement for the simultaneous operation of the scientific and service systems of the spacecraft (SC), such as service onboard radios (OE CMC), transmitters of the highly informative channel of scientific data (VIRK), and onboard high-sensitivity radio astronomy receivers in the frequency range of 300–26000 MHz. Tests on this problem within the requirements were carried out partly during radio astronomy checks (RAC) at a special landfill of the Pushchino Radio Astronomy Observatory (PRAO), partly within the program of the experimental ground testing of the OSE at the Astro Space Center of Physics Institute (ASC PI) in Moscow, and finally during factory tests of the space complex at NPO Lavochkin [1].

In Moscow, it was proposed to test the interferometer with a zero base (ZBI-0). The main feature of the tests was that the radio interferometer was made up of two arms. The onboard arm consisted of the OSE SRT, and the ground arm consisted of the GRT with equipment from ground radio telescopes. The test signal was fed on inputs of ZBI-0 arms. It had no natural time lag typical of the signal from space radio sources at the inputs of the real interferometer (with geometrically spaced arms). It determined the test name. In test of the ZBT-0 whole system is in a static condition and practically designed to determine the compatibility from onborne and ground-based scientific data. In these tests we tested the operation of the correlator and scientific data recorder, developed in the ASC for processing jnboard and ground-based scientific experimental data. During ZBI-0 tests important results on the operation of individual systems were obtained that determined the technology of tests of the ZBI-0 and the space radio telescope as a whole. A significant drawback of ZBI was the lack of the part of the equipment (for obvious technical limitations) of the antenna of the radio telescope, although it did not detract from the importance of the test.

2. EXPERIMENTAL

The diagram of ZBI-0 is shown in Fig. 1. It should be noted that in this diagram there is no transmission line of scientific data from the spacecraft to the ground tracking station (GTS). This question was studied independently, as part of the reliability of signal transmission by VIRK radio line, and the analysis showed the validity of the construction of the test setup shown in Fig. 1. The diagram shows the correlation parameters of the signals, namely autocorrelation (AC), interchannel (IC), and cross-correlation (CC), used in the verification of the interferometer in different wavelength ranges. As the most simple in terms of technology, ZBI-0 tests were started with a range of 6 cm.

In section II (Fig. 1) there are two signals fed to ZBI-0 arms. The main noise-like signal from the noise generator (NG) with the adjustable output level, and a second dial tone, 4828 + 3.2 MHz, was applied in order to monitor the correctness of the test setup assembly. When properly assembled, there should be a 3.2 MHz signal correlation spectra of the upper sideband.

The signals at the output of the interferometer arms should be compatible in order to carry out their correlation processing. Therefore, the device DAS, specially designed at in *British Aerospace* was used in the ground arm of the interferometer. This device forms the required format of scientific data S2, which are recorded on a digital recorder RDR. In the space–

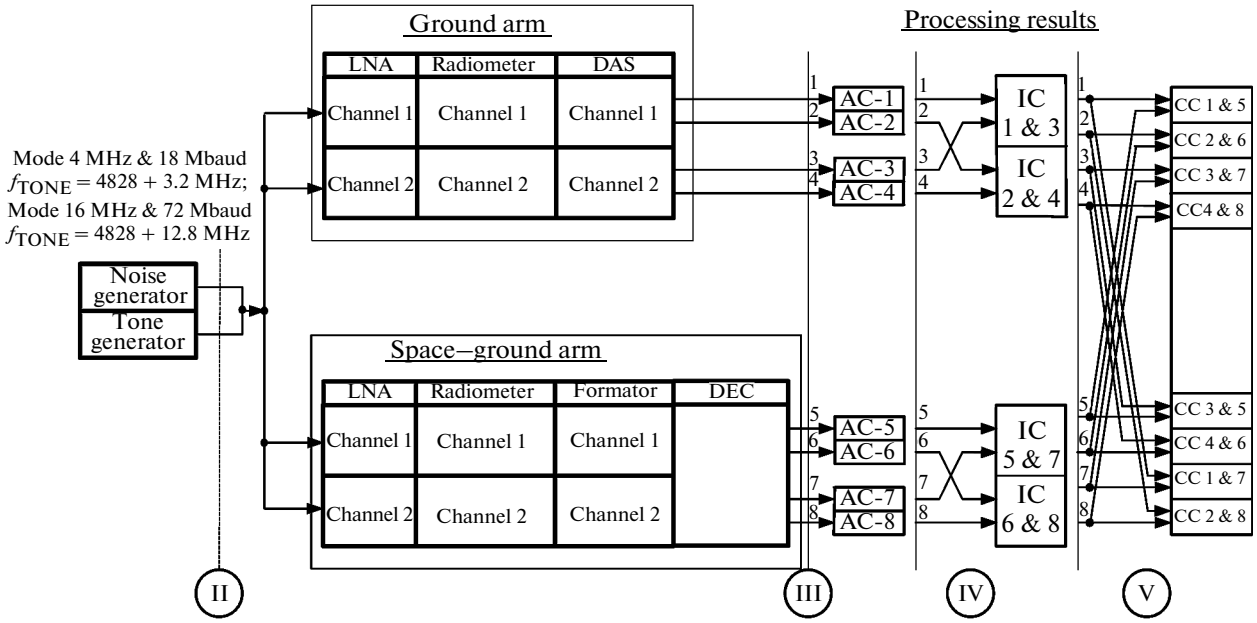

Fig. 1. The ZBI-0 test setup.

ground arm the end portion is more complicated. Ship scientific data come on the onboard unit Formator in the analog form. The frequency inverter (FI) signal spectrum is converted into four video bandwidths of 16 or 4 MHz, digitized, and represented as a "parallel" digital data stream. This stream is then condensed into a high-speed "serial" stream of digital data and is used as a signal modulating a carrier frequency of 15 GHz of VIRK that transmits scientific information to the ground. The modulated signal received at the ground is correspondingly processed at the GTS and is fed to the input of the ground device Decoder, which converts spaceborne signals from the serial into the parallel digital stream S2 (as well the stream at the ground arm), and then is fed to the digital recorder RDR. As already mentioned, the ZBI-0 diagram does not actually have the VIRK interferometer arm segment ("modulator–radio emission–radio line–receiver–demodulator). This feature was specifically incorporated into the OSE at the initial design phase of the RadioAstron mission in order to simplify the testing technology.

Ultimately, both spaceborne and ground signals recorded on RDRs make it possible to obtain autocorrelation and cross-correlation characteristics of the interferometer after their playback and appropriate processing. These characteristics quite adequately reflect the properties of the radio interferometer in general and its arms in particular.

Figure 1 shows conditional sections:

(1) Section III. It is possible to obtain autocorrelation functions (ACF) and autocorrelation spectra (ACS) of the interferometer.

(2) Section IV. It is possible to obtain the so-called interchannel correlation functions (ICF) and interchannel correlation spectra (ICC) of the interferometer.

(3) Section V. It is possible to obtain cross-correlation functions (CCF) and cross-correlation spectra (CCS) of the interferometer.

Further, the analysis of the ZBI-0 test results for the two year period showed the stability and repeatability of AC, IC, and CC results. Since in a real experiment there are various ground arms, the technical project management considered it appropriate to simplify the ZBI-0 test setup of in the final stage at the NPO Lavochkin and use IC parameters only.

3. CALIBRATION TESTS

First, the problem of determining the sensitivity of the radio interferometer associated with the signal decorrelation and the maximum achievable time of the coherent accumulation was introduced into the range of experimental problems of the ZBI-0. Since interferometer sensitivity is a value which depends on many factors, it is reasonable to represent these relationships graphically and note the limitations in the form of numerical values in the graphs. Thus, the plot shown in Fig. 2 was obtained. There, two curves are plotted on the same graph with a single digitization:

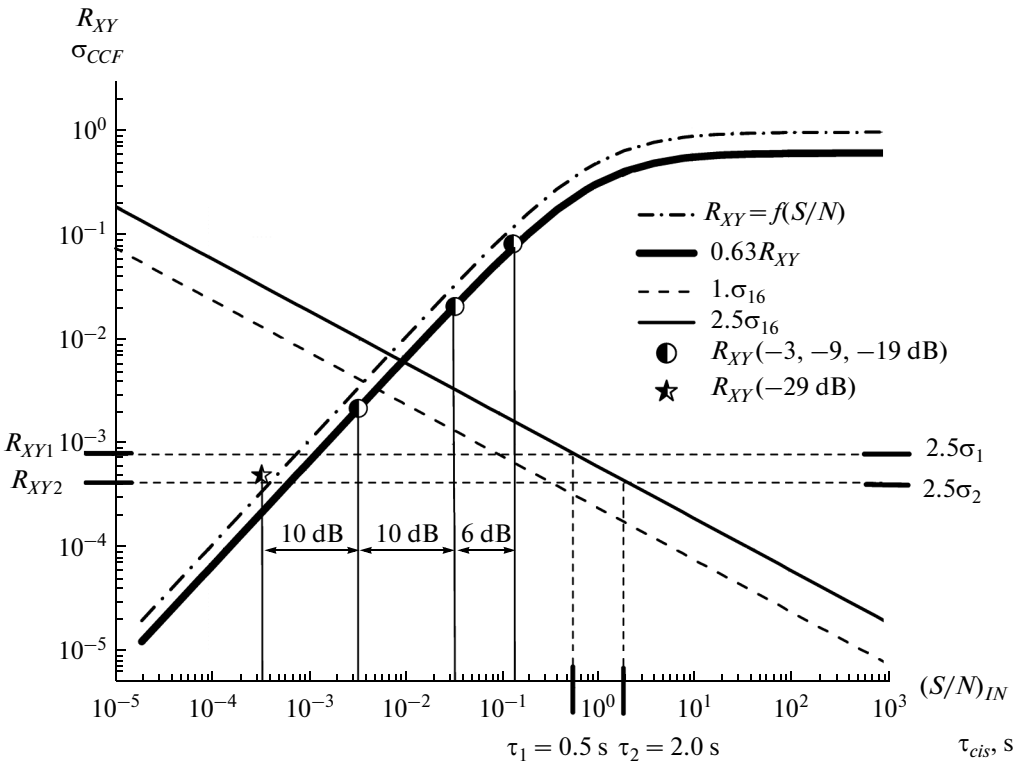

Fig. 2. Plot for amplitude calibration of interferometer.

(1) The value of CCF (R_{XY}) depending on the radio engineering signal/noise ratio at the receiver input, where $S_{in} = S_{cog}$ is the equivalent power of a noise-like signal from a radio source at the input of the interferometer and $N_{in} = S_{uncog}$ is the equivalent noise power at inputs of interferometer arms, is

$$S_{in} = \sqrt{\frac{S_{in1}^2 + S_{in2}^2}{S_{in1} \cdot S_{in2}}},\ N_{in} = \sqrt{\frac{N_{in1}^2 + N_{in2}^2}{N_{in1} \cdot N_{in2}}},$$

$$R_{XY} = \frac{S_{in}}{S_{in} + N_{in}} = \frac{S_{cog}}{S_{cog} + N_{cog}},\ \sigma_{ccf} = \sqrt{\frac{1}{\Delta F \cdot \tau_{cis}}}.$$

The dot–dash line in Fig. 2 show the calculated dependence $R_{XY} = f(S/N)$, and the bold solid line below and parallel to it is the dependence $R_{XY} = 0.63f(S/N)$, taking into account one-bit quantization.

(2) The dashed straight line descending from left to right shows the dependence $\sigma_{ccf}(\tau_{cis})$ for the video channel bandwidth of 16 MHz, and above it there is a parallel solid line $2.5\sigma_{ccf}(\tau_{cis})$. If the CF value exceeds $2.5\sigma_{ccf}$ (as a "convolution" of bilateral intrinsic noise 5σ), it indicates the presence of coherent signals in correlated streams.

For example, for the given parameters of video paths of the interferometer and at $\tau_{cis} = 0.5$ s the CF (R_{XY1}) is determined with an amplitude above $8 \cdot 10^{-4}$ (R_{XY2}) (the upper horizontal dashed line), and at $\tau_{cis} = 2.0$ s, more than $4 \cdot 10^{-4}$ (the lower horizontal dashed line).

The following test was carried out, in order to carry out the amplitude calibration using the proposed plot.

The signal NG was selected for the test so that the CF value fell at the end of the linear portion of R_{XY} (before the nonlinear portion on the right, upper point). At this level of the test signal, it is possible to visually identify the signal/noise ratio on the screen of the spectrum analyzer and, thus, to ensure reliable values.

Further, calibrated fixed attenuators were introduced in turn in the test setup, and the ASL correlator was used to process recorded signal/noise ratios in order to obtain CF values. In Fig. 2, these values are denoted by half-solid circles. The values of attenuators used are also indicated.

Diagrams of consecutive test steps are shown in Fig. 3 (left column of the figure). For the top two diagrams the NG signal was fed to both arms of the interferometer, in which CF ≅ 0.08. The signal is strong, the correlation noise in the lower sideband (LSB) is not visible, and in the upper sideband (USB) the stand from the tonal signal of +3.2 MHz is visible. On the third from the top diagram, after the introduction of 6 dB at the attenuator input, amplitude of the CF decreased by four times and amounted to ≅0.022. Small noise appeared at the base of the CF. On the fourth diagram after the introduction of additional 10 dB the CF became ≅0.0024 (decreased by 10 times) and the CF noise became noticeable. At the last fifth diagram after the introduction of 10 dB of attenuation in the NG cir-

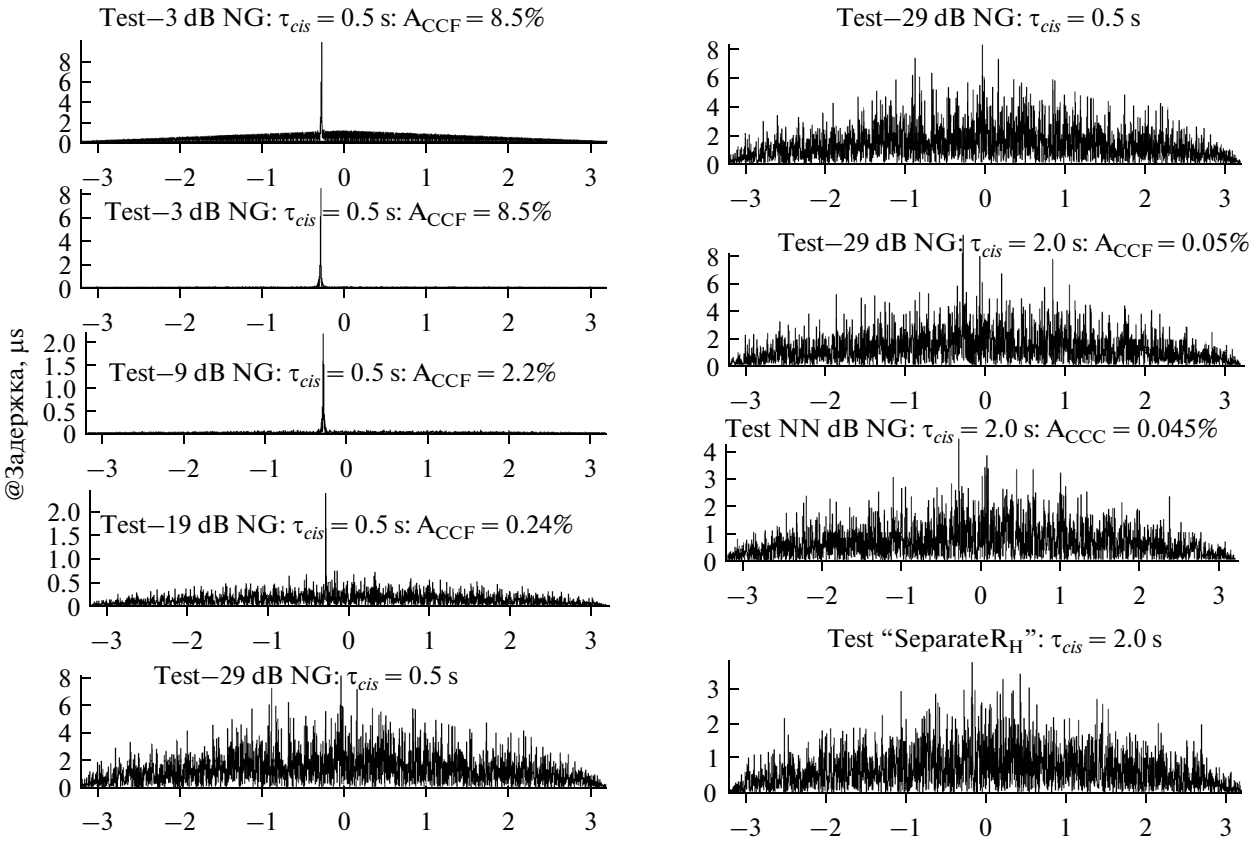

Fig. 3. Cross-correlation functions for amplitude calibration of interferometer.

cuit, the CF could not be determined because the CF noise covered the corresponding point R_{XY}.

The above-mentioned diagrams were obtained at the time of coherent accumulation τ_{cis} = 0.5 s. The presence of a maximum shear of the CF maximum on diagrams is explained by the difference in instrumental delays in interferometer arms, being about 3 μs and stored in all the experiments with this set of equipment. The obtained results fit well on the plot, the last point at the 29 dB attenuator is below the level of $2.5\sigma_{ccf}(\tau_{cis}$ = 0.5 s), which corresponds to CF drop outs in noise. The noise reduction to the edges of diagrams is associated with the correlator type. Here by the edges of the determined window of delays the number of samples involved in the correlation is reduced.

The same data were processed for the coherent accumulation time τ_{cis} = 2.0 s (see diagrams in the right column of Fig. 3). For comparison, the upper diagram in this column repeats diagram 5 in the left column (τ_{cis} = 0.5 s). On the second right diagram at τ_{cis} = 2.0 s the CF appeared with an amplitude of 0.0005. Compared with the plot data, the value is somewhat overestimated. When NG is disconnected (diagram 3, the right column), the CF amplitude is 0.00045. However, this nonsubjective determination of the value sin*X*/*X* of the CF amplitude, like all the previous ones, is obtained by a digital hardware-based method and is recorded in diagram titles (unfortunately, they are not legible in the text of the diagrams). The location of points and noise levels on the plot shows that for the current value of R_{XY} and adopted τ_{cis} = 2.0 s it should be possible to determine the CF on the diagram, which is actually true (the sign above the level of $2.5\sigma_{ccf}(\tau_{cis}$ = 2.0 s).

As it turned out, the overestimation of the measured values at low levels of input signals is because there is not enough isolation between the inputs of the interferometer arms during testing located at the level of 1/0.00045 = 2222 (this is more than 30 dB). The increase of the isolation between inputs is associated with technical difficulties when dealing with weak signals and the need to increase the power of the test generator. The insufficient isolation is confirmed by diagram 4 in the right column. In this test, the input signal supply unit was turned off, and only independent matched loads of 50 ohms were left. There is no CF signal.

In the calibration of the interferometer the test-signal circuit is shown in Fig. 4. The introduction of valves with the reverse attenuation of 40 dB into the setup was an important improvement, although it was made after the described tests.

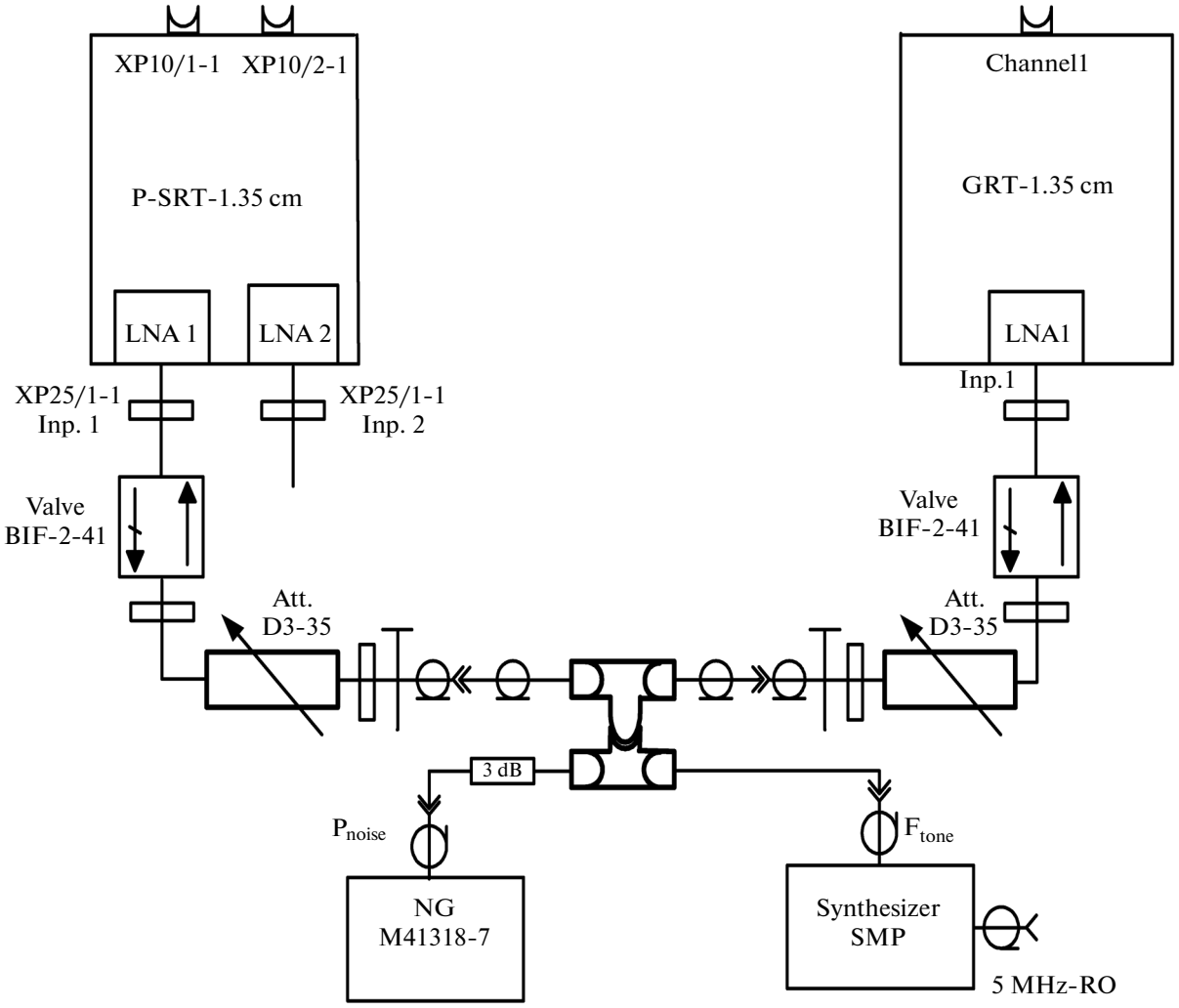

Fig. 4. Signal circuit in the ZBI-0 for a range of 1.35 cm.

In the plot in Fig. 2 it was supposed that R_{XY} is constant over time. However, in fact it is not. Firstly, there is a generator signal-coherence time associated with intrinsic phase noises of the device. This time decreases as the nominal frequency of the device increases, since the absolute phase fluctuation increases at a constant relative frequency stability. There is a rough estimate of the time coherence

$$2\pi f_0 t_c \sigma_y(\tau_c) \cong 1.$$

The time coherence is conditionally equal to the time t_c, for which the mean square error of the phase at the appropriate $\sigma_y(\tau_c)$ can reach 1 radian. The plots of the decorrelation of signals shown in Fig. 6 are made according to available data of the Allan variation (ADIV) (Fig. 5).

The curves show that the signal decorrelation does not pose any problems, if the onboard arm of the hydrogen frequency standard OHFS-SRT in the range 6 cm is used as the reference oscillator. This value is

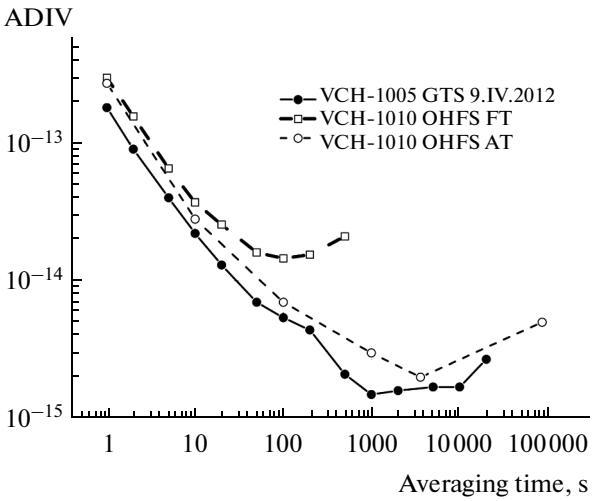

Fig. 5. Allan variations for OHFS and GHFS.

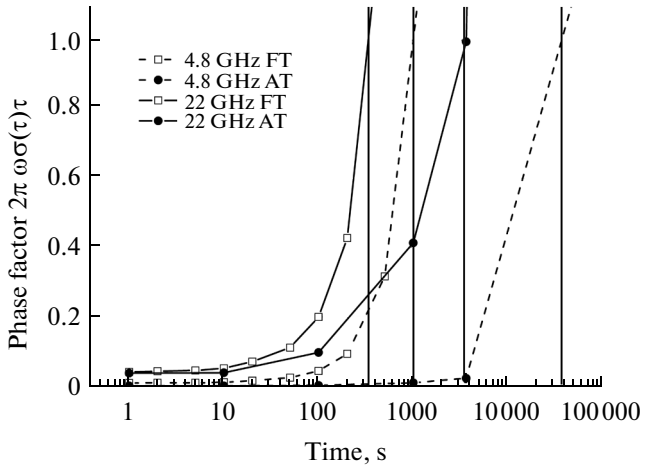

Fig. 6. Signal decorrelation time in ranges of 6 and 1.35 cm.

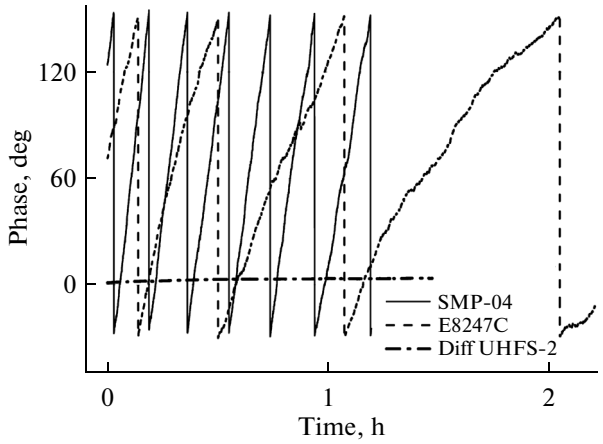

Fig. 7. The frequency shift and phase drift of heterodyne signals at 4320 MHz.

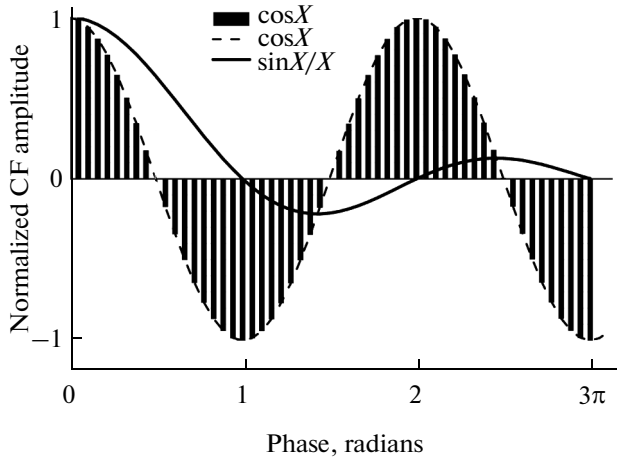

Fig. 8. The ratios of instantaneous and average CF values.

more than 10000 s, which in practice is not used in interferometry. In the range of 1.35 cm the situation is tenser, because in the case of the consideration of the onboard hydrogen two Allan variations are possible, which are shown in Fig. 6:

(1) The curve obtained for acceptance tests (AT) by the manufacturer (indicated by the filled circles).

(2) The curve obtained for complex tests (CT) at NPO Lavochkin (denoted by contour squares). Frequency drifts affect the minimum of ADIV characteristics and their slope to the right of this minimum. It is known that in CTs the OHFS was not provided with the required heating because of technological reasons, but these results of ADIV CTs were published and, thus, the result should be explained. According to ATs, the decorrelation time is ~4000 s, and according to CT it is ~400 s. As can be seen from the ADIV graphs, the long-term warming of OHFS significantly increases the decorrelation time of the reference signal. According to the results of flight tests (FT), after two years of continuous operation the type of ADIV OHFS is the same as the ADIV GHFS on the tracking station.

As shown by numerous tests, frequency drifts of insufficiently warmed devices in the radiointerferometer lead to results similar to the results of CTs. One of the sources of such drifts is frequency synthesizers widely used in interferometer arms. Figure 7 shows the relative progress of the signals of conversion frequencies of 4320 MHz formed based on a single reference frequency in the frequency synthesizer of OGHCF-SRT and two industrial synthesizers. Each period of the sawtooth signal in the plot in Fig. 7 corresponds to a phase change of the measured signals by π (180°). If the signal of the synthesizer Agilent E8247E (dashed line) has an offset $\Delta f/f_0 = 3.2 \cdot 10^{-14}$ and this value decreases with the heating, the signal of the synthesizer SMP Rode & Schwarz (solid line) is shifted about $\Delta f/f_0 = 1.8 \cdot 10^{-13}$ and varies slightly, i.e., there is a constant frequency shift. The comparison of the signals of OGHCF-SRT shows a slight frequency shift of less than $\Delta f/f_0 = 1.0 \times 10^{-15}$. Below, when considering the shift of video bands, such displacements will be estimated.

The impact of frequency shifts of the studied spectra at the ZBI is confirmed by measurements in the ZBI-0. As is known, if both arms are synchronized by the same reference signal, the coherent accumulation time for the signal (τ_{cis}) is almost unlimited. When using separate reference signals in interferometer arms, a shift of reference frequencies occurs. As a result, shifts of studied video spectra take place. The problem of the shortage of τ_{cis} caused by the limitation of the accumulation time of mean obeying the law of sinX/X manifests itself (Fig. 8). The graph shows that mean sinX/X is the function of only the relative phase of correlated signals.

Figure 9 graphically illustrates the relationship of time τ_{cis} on the frequency of the studied range and on the relative magnitude of video band shifts by frequency. In this figure, the function sinX/X calculated

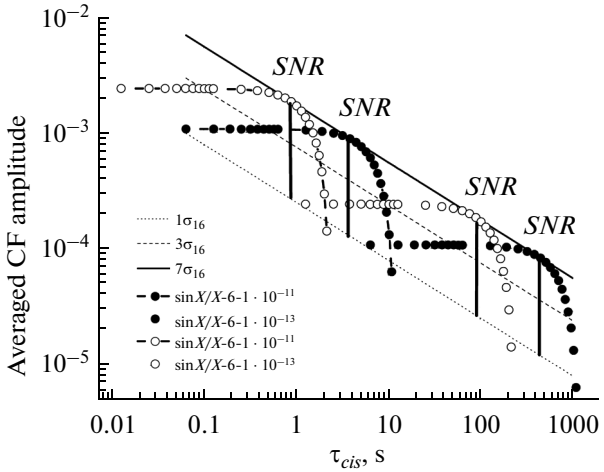

Fig. 9. Average CF value in ranges of 6 and 1.35 cm in the case of reference frequency (RF) shift $1 \cdot 10^{-11}$ and $1 \cdot 10^{-13}$.

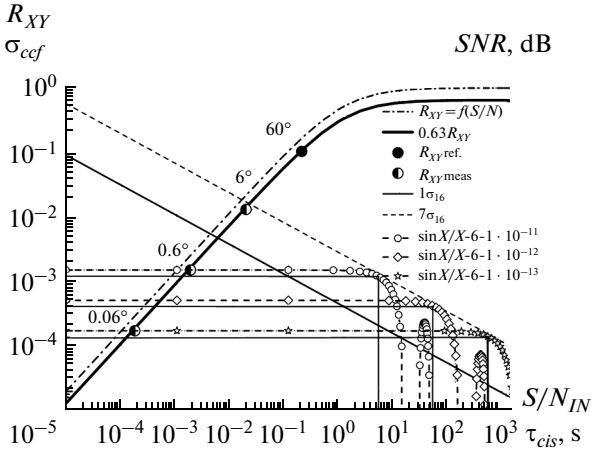

Fig. 10. ZBI-0. Plot for determining TCC in 6-cm range.

and normalized by the CF maximum for frequency bands 6 and 1.35 cm, as well as for relative shifts of reference frequencies $1 \cdot 10^{-11}$ and $1 \cdot 10^{-13}$, is shown on a logarithmic scale. It can be seen that by reducing frequency shifts it is potentially possible to increase interferometer sensitivity by increasing coherent accumulation time.

It is desirable to have a signal/noise ratio at the correlator output of $SNR = R_{XY}/\sigma_{ccf} = 3\text{–}7$, where $\sigma_{ccf} = 1/\sqrt{\Delta F \cdot \tau_{cis}}$, ΔF is the video channel band, Hz; τ_{cis} is the accumulation time, in seconds; *SNR* is the exceedance of R_{XY} over correlator noises. Usually, the value of *SNR* is represented in times or decibels. It should be noted that sensitivity is often uniquely associated with the *SNR* value and is used as a measure of interferometer sensitivity $SNR = R_{XY}/\sigma_{ccf}$.

On the plot (Fig. 9) it is not difficult to find the set of the same values of *SNR* that correspond to different values of S/N_{in} and τ_{cis}. In reality, interferometer sensitivity grows because of increasing R_{XY}, and this is a technical description of the receive path. The decrease of $\sigma_{ccf}(t)$ is a function of time that makes it possible to see the CF against its background of its internal noise (if the requirements for the signals mentioned above are met). It means that the parameter *SNR* cannot be used as a measure of interferometer sensitivity.

Therefore, when discussing the problems of the interferometer sensitivity, in the first place, it is necessary to take into account the internal noise of radiometers, then at the maximum available time of coherent accumulation or time of decorrelation (whichever occurs sooner) it is possible to determine the maximum sensitivity. The plot shown in Fig. 10 most fully reflects a situation with several variable parameters of the interferometer and directions of their variations for the maximum CF for a particular interferometer.

4. MODIFICATION OF TESTS

The qualitative development of the measuring equipment made it possible to reduce the amount of equipment involved in the tests without compromising the quality of the measurements. In real SRT tests, it was attempted to substitute the second arm of the interferometer by extending test session time. As a result, a virtual interferometer was obtained with options that were specific to one of its arms, in this case, to the arm OSE-SRT. This operation was correct when testing with the use of generators of harmonic input signals (those signals are quasicoherent in time). The appearance of the equipment with the formation of the coherent pseudo noise sequence (CPNS) simplified the ZBI-0 test setup and made it possible to abandon the supply circuit of test signals in the two arms of the interferometer, which is especially attractive when tested in the range of 1.35 cm, which requires the use of waveguide technology. This simplification proved to be strategically correct, because previous trials involved the second arm with its settings that had a corresponding impact on the final result. More importantly, in the actual situation on the RadioAstron project there is a set of second (ground) arms. It is almost impossible to test them under the ZBI-0 mode. At the same time, it is possible to test ground-based telescopes under the ZBI-T mode (for the identification of the arm test mode with CPNS signals with the extension in time the notation ZBI-T was introduced, where T is time). In such a situation the comparison of characteristics of radio telescopes becomes more objective.

The results of the interferometer calibration in the range of 6 cm using ZBI-T are shown in Fig. 11. The first thing to note is a more accurate calibration (compared with the calibration of Fig. 2) and a larger dynamic range. The second important thing is that there are no spurious signals that disrupt the linearity

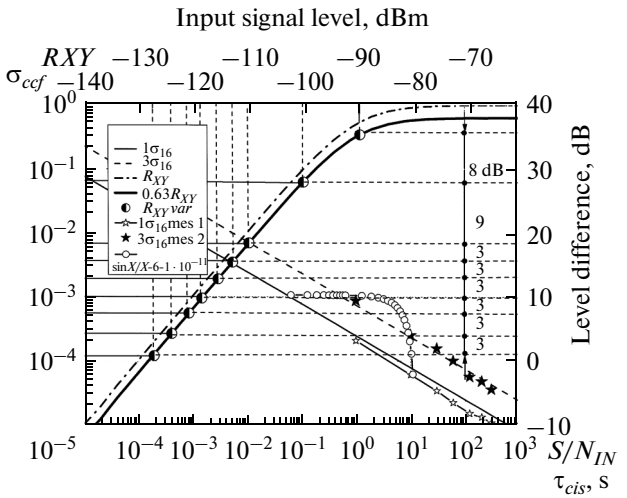

Fig. 11. ZBI-T. The calibration of ground receiver of 6-cm range by coherent PNS signal.

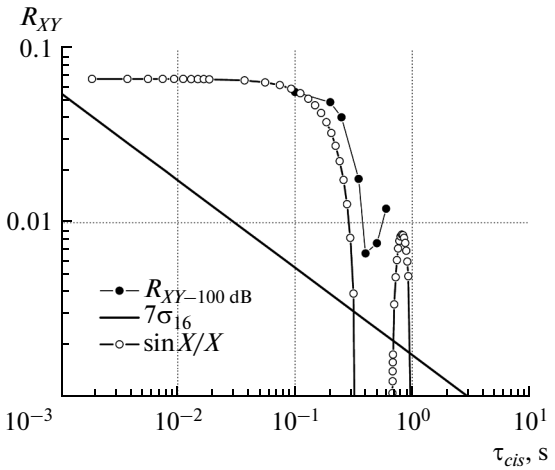

Fig. 12. ZBI-T. The TCC in range of 6 cm in the case of the RF shift $3.1 \cdot 10^{-10}$.

of the function R_{XY} in the same area. The selection of times of the coherent accumulation is fully consistent with the plot data. $\sigma_{ccf}(t)$ is measured by both methods, but the results are close to those calculated and are beyond question.

The further development of the ZBI-T measurements made it possible to show on the plot the influence of the frequency shift on reference generators. For this purpose, two records of PNS signals were made. One of the records was made using the reference signal from the OHFS, while the other was made using a reference signal from the onboard rubidium frequency standard (ORFS). The interval between measurements simulated the frequency drift during this interval. Previously, from the condition of the processing time minimization the relative frequency shift of the reference oscillator (RO) was determined. It was $3.1 \cdot 10^{-10}$. On the plot in Fig. 12 the curve with solid dots shows measured values, while curves with empty dots indicates calculate values. Qualitatively, the effect was fully confirmed. It was not possible to completely confirm it from the quantitative point of view due to lack of time. In order to increase accuracy, it is necessary to select processing parameters and to increase the number of experimental points by at least an order of magnitude.

All the above, presented as illustration, was mainly based on tests in the range of 6 cm as the most technologically advanced and sufficiently high frequency. In the RadioAstron mission the range of 1.35 cm is much more difficult, since it is divided into eight bands in increments of 960 MHz band and has a common band from 18 to 26 GHz. A device that is equivalent to eight separate receivers is necessary in order to conduct tests. These tests were focused on the stability of the parameters of the phase characteristics of paths and the stability of the coefficients of the transmission of paths in short time intervals of a few minutes but that could be traced throughout 2–3 years. The center of gravity in the testing of the receiver was in the range of 1.35 cm, F0 (the central frequency of 22 232 MHz).

Figure 13 shows the results of the cross-correlation processing of the two-minute test session of February 9, 2007, 09:38:50–09:40:50 on the new generation ASC correlator. The test was performed by the method of ZBI-0 and for the common reference oscillator (CRO). Five standard (for the ASC) parameters were given for evaluating the performance of the device in the session:

1. The CCF amplitude curve (Ampl) for the upper (USB) and lower (LSB) sidebands. The shift between the curves estimates the phase and partly the amplitude channel identity, while the parameter-value change measures the stability of the channel per session.

2. The graph of the real part of the CCF (Re.part) makes it possible to determine whether these are phase or amplitude problems arising in the path by comparing with the CCF amplitude.

3–4. Two phase indicators with an overlap interval $-\pi\ldots+\pi$ (Phase + −) and $0–2\pi$ (Phase +) make it possible to exclude from consideration the phase transition regions on the borders $N \cdot 2\pi$ and $N \pm \pi$ (simply for convenience), and to determine spectra shifts by frequency and frequency stability by the slope and curve fluctuations. Thus, for this test we have:

(1) The eigen frequency shift in the channels $\delta f = 25°/2/22232000000/360/120 = 1.3 \cdot 10^{-14}$.

(2) The stability of $\sigma_f = 25°/22232000000/360 = 3.12 \times 10^{-12}$ for $\tau_{cis} = 1$ s.

(3) The coherent accumulation time τ_{cis} limited by the spaceborne radio system is about 4000 seconds. The possible deterioration of this parameter depends on the parameters and mutual settings of the ground arm of the interferometer.

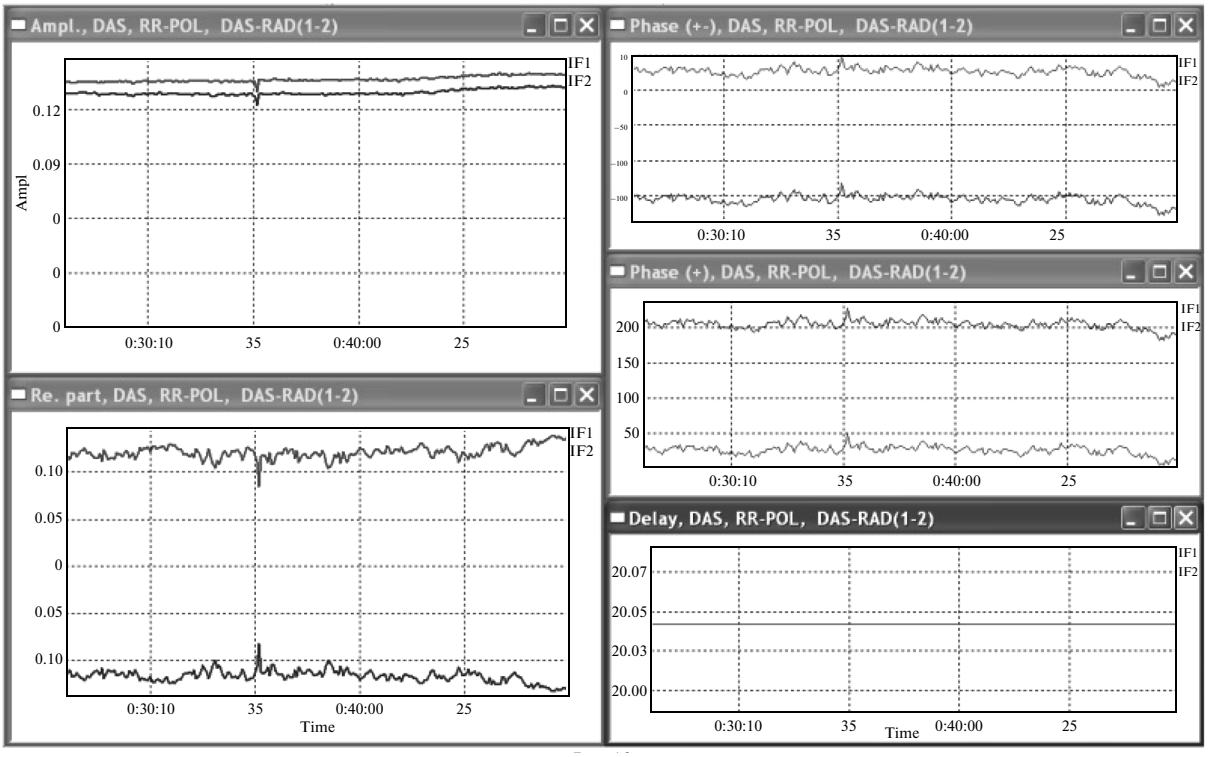

Fig. 13. Main characteristics of interferometer obtained by correlation processing.

(4) The phase shift π between USB and LSB is caused by circuit design problems in the implementation of onboard generator of sidebands *SSB* as well as the value of Re.part4 symmetrical with respect to 0.

5. As mentioned above, the graph of the current signal path delay is about the order of 3 μs for the given set of equipment of the ZBI-0 and is stored in a stable condition.

These are good characteristics for the range of 1.35 cm, F0. Similar characteristics are observed for the other bands F-4–F3.

The stability of interferometer parameters in the range of 1.35 cm at long time intervals. Parameters of receivers were measured periodically for several years. In the end, it was possible to plot a joint graph. This graph shows only measurement results obtained at the ASC, before transferring the complex to NPO Lavochkin (October 2009), and at NPO Lavochkin, before transferring the set to the final assembly (February 2011). The averaged graph is not shown on purpose, because it would only obscure the overall picture. As mentioned above, the analysis of total measurements of AC, IC, and CC at the initial stage of the ZBI-0 made it possible to conclude that measurements of the IC only, which were also carried out within ZBI-T, could be stopped.

According to the measurement results (Figs. 14 and 15) yet another important conclusion was made that the waveguide polarization splitter at the input of the low-noise amplifier (LNA) of 1.35 cm was narrowband one. Initially it was set up to operate in the range of 1.35 cm, F0 (IC tends to 0), but due to the drift from this frequency IC values began to grow, which was apparently because of the decrease in the interchannel damping for polarization channels.

CONCLUSIONS

As a result, a number of characteristics and parameters of the equipment complex of the space–ground radio interferometer were obtained in test modes ZBI-0 and ZBI-T. Basically, definitions referred to the spaceborne arm as a new phenomenon in interferometry on very large scale bases, although many of the provisions can be common to all interferometers.

It is well-known that in radio interferometry the requirements for characteristics and parameters increase with the frequency of the signals. Therefore, when testing equipment of the RadioAstron mission, ranges of 6 and 1.35 cm were preferred, and the ranges of 92 and 18 cm were considered normal (for interferometry), unless there were any problems on the upper ranges.

Two methods of testing were used for the study:

(1) The classic ZBI-0, where the two arms of the interferometer are tested at the same time, the same test signal is fed at inputs, and the result is evaluated by the calculated CF.

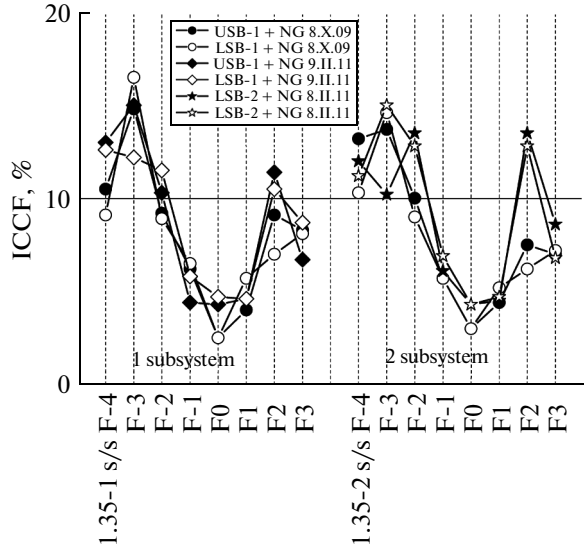

Fig. 14. ICCF of 1.35-cm range during tests of the OSE (with the NG feed).

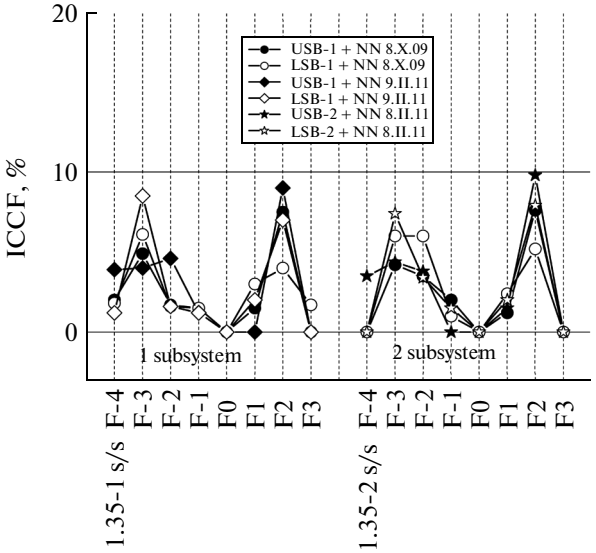

Fig. 15. ICCF of 1.35 cm during tests of the OSE (without NG feed).

(2) The upgraded ZBI-T, where only one arm of the interferometer is tested, the test signal is applied twice with a time shift, and the results are assessed by the computed ICF.

The calibration of radiointerferometers consists in the comparison of the calculated and experimental CF values. Calibrations in the range of 6 cm by the method of ZBI-0 and in the range of 1.35 cm by the method of ZBI-T were carried out. Results were the same in terms of accuracy and are ~10–15%. The dynamic range of test signals in the ZBI-T mode was wider because in this method there was the insufficient amount of interchannel isolations.

The coherence time of the signals is one of the most important factors that limits the potential interferometer sensitivity. According to the Allan variation for the reference signal, which is the basis for the formation of signals involved in frequency conversions in interferometer arms, the coherence of the signals should be maintained within 4000 s for the range of 1.35 cm and within more than 10000 s for the other bands.

The second factor that limits the interferometer sensitivity is the frequency shift of transformed spectra that results from the inaccuracy of setting nominals of reference signals in the interferometer arms and because of spacecraft motion with respect to the GTS (the uncertain knowledge of the orbit, occurrence of relativistic corrections, as well as ionospheric and tropospheric shifts). Depending on the magnitude of the frequency shift of the RO and used bandwidth of the interferometer the average value of the accumulated signal falls and at some point it becomes comparable to the correlator internal noise. This time interval will determine the time of coherent accumulation (TCC).

It is proposed to specifically assess the current situation using a plot having parametric graphs σ_{ccf} as time functions, bands of the analyzed signal, selected multiplicity σ, and correlation function travel depending on the relative frequency shift of video spectra. With these data it is possible to determine the expected value of R_{XY} and the TCC necessary for it or vice versa.

The influence of frequency drifts of reference signals on the Allan variation curve was established. In particular, for the range of 1.35 cm when switching to the operating mode, if the onboard frequency standard is poorly warmed up, signal coherence time decreases to ~400 s vs ~4000 s after a long warm up (several days). Similarly, frequency drifts in the equipment lead to a decrease in the coherence time.

During the ZBI the long-term stability of ICF parameters, which are measured over several years, was confirmed. The ICF were given for the completion of tests at the ASC in 2009 and at NPO Lavochkin in 2011. Averaged characteristics were intentionally not shown. There is a good repeatability of results at the ~±15%, which indicates the stability of the reception paths of the interferometer.

These graphs also show the rise in ICF values during the transition to the edges of the total range of 1.35 cm. Apparently, this is due to the bandlimitedness of the waveguide polarization selector, and that it was originally designed and optimally tuned for the frequency of 22 232 MHz.

One more argument in favor of the opinion of the narrowbandness of the polarization selector is that without the test signal, the ICF is close to zero at the frequency F0 and increases on adjacent frequencies. It is possible to assume that this pattern depends on the setting of the unit of antenna irradiators at 1.35 cm,

namely due to the deterioration of the crosstalk on frequency channels adjacent to F0 and interpenetration of the test signal in the polarization channels of receivers that increases the CF value.

The first obtained correlation functions of signals in the ZBI-0 mode can be dated to the beginning of 2000. The correlation proved to be cumbersome and poorly controlled. At the same time, the optimization and minimization of obtaining of correlation characteristics began at the ASC. As a result, the recording of scientific data on hard disks was developed, the algorithm for the onboard creation of the compressed data stream was revised, ground scientific data decoder was redesigned, and some other innovations were made. At the same time, new elements of advanced metering technology with coherent pseudonoise output signals were introduced in the test method ZBI-0 that made it possible to move away from the "classical" testing of ZBI-0 in favor of "temporary" ZBI-T. At first, such an approach hindered the testing but eventually it made it possible to make rapid speed in the final stage of testing and compensate for the resulting lack of time.

All the above arguments were checked during the tests, and the obtained experimental data confirmed the operation of the radio electronic complex of the interferometer correct from the point of view of radiotechnics. The obtained characteristics were uniquely interpreted and ready to use for calculations in the field of astronomy.

As a result, the ZBI took more than 10 years of preparatory work and tests, redesign and production of a significant amount of new equipment, interpretation of the results, and repeated tests for technological and flight models of onboard instruments and ground equipment. Thanks to the great work carried out by the staff of the ASC, Space Research Institute, related manufacturers of individual devices, a huge staff of NPO Lavochkin in preoperational and flight tests, the ZBI project was successfully completed. Individual test items were borrowed to the electromagnetic compatibility (EMC) testing program for the whole automatic channel check (ACC) complex. Today, when the satellite has been operating in orbit for more than three years, it can be argued that the tests were carried out efficiently. It should be noted that the record characteristics of the space–ground radio interferometer alleged in the early stages of the project were implemented in practice largely thanks to new technical solutions in the design and testing of the interferometric complex, as well as to the dedicated work of the team of scientists, engineers, and workers involved in the implementation of the RadioAstron mission.

REFERENCES

1. Kardashev, N.S., Radioastron (project "Spektr-R") – A radio telescope much larger than the Earth. Basic parameters and tests, *Vestnik NPO im. S.A. Lavochkina*, 2011, no. 3, p. 11.

Translated by O. Pismenov